in detail. The result is that the same upper bound as before is required for k_V, but the lower bound on h decreases as the number of vehicles taken into account by the controller increases.

iii) For the bi-directional control strategy, platoon stability is ensured without any restriction on the time headway, but the results for jerk limitation depend on whether or not the transfer functions corresponding to the look-ahead and look-astern aspects are identical. In the symmetrical case, the previous upper bound on k_V is again required, and when combined with the requirement of collision avoidance, it imposes a lower bound for the inter-vehicular spacing which is dependent on the length of the platoon, although independent of the speed. This constraint, however, appears to be avoidable in the asymmetrical case with $k_{V+} = 0$, where the jerk limitation bound is replaced by a similar one on k_P/k_{V-} if $k_{V-} \gg \sqrt{k_P}$ and the control parameters for the last vehicle in the platoon are appropriately chosen. The condition obtained for collision avoidance is then compatible with the other constraints required, provided that the parameters in the control laws are allowed to take arbitrarily large values.

It is not, of course, obvious that conclusions of the kind obtained here will remain valid when more realistic models are considered, especially with nonlinear effects being explicitly taken into account. Indeed, even in the linear case, introducing a time lag between the control signal and the consequent acceleration, via (3), can result in a lower bound on the headway being necessary for string stability [8]. Nevertheless, the simple treatment given here may at least serve to indicate what can be expected to be found from a more general investigation.

REFERENCES

[1] P. A. Cook and S. Sudin, "Dynamics of convoy control systems," in *Proc. 10th Mediterranean Conf. Control Automation*, Lisbon, Portugal, 2002, pp. WP7–2.

[2] P. A. Cook and S. Sudin, "Convoy dynamics with bidirectional flow of control information," in *Proc. 10th IFAC Symp. Control Transportation Systems*, Tokyo, Japan, 2003, pp. 433–438.

[3] J. Eyre, D. Yanakiev, and I. Kanellakopoulos, "String stability properties of AHS longitudinal vehicle controllers," in *Proc. 8th IFAC/IFIP/IFORS Symp. Transportation Systems*, Chania, Greece, 1997, pp. 69–74.

[4] C. Y. Liang and H. Peng, "Optimal adaptive cruise control with guaranteed string stability," *Veh. Syst. Dyna.*, vol. 32, pp. 313–330, 1999.

[5] L. E. Peppard, "String stability of relative-motion PID vehicle control systems," *IEEE Trans. Autom. Control*, vol. AC-19, no. 5, pp. 579–581, Oct. 1974.

[6] R. Rajamani, H. S. Tan, B. K. Law, and W. B. Zhang, "Demonstration of integrated longitudinal and lateral control for the operation of automated vehicles in platoons," *IEEE Trans. Control Syst. Technol.*, vol. 8, no. 4, pp. 695–708, Jul. 2000.

[7] S. Sheikholeslam and C. A. Desoer, "Control of interconnected nonlinear dynamical systems: The platoon problem," *IEEE Trans. Autom. Control*, vol. 37, no. 6, pp. 806–810, Jun. 1992.

[8] S. Sudin and P. A. Cook, "Effect of vehicle dynamics on vehicle convoy system stability," *IEEE Trans. Intell. Transport. Syst.*, 2007, submitted for publication.

[9] D. Swaroop, "String stability of interconnected systems: An application to platooning in automated highway systems," Ph.D. dissertation, Univ. California, Berkeley, CA, 1997.

[10] D. Swaroop and J. K. Hedrick, "String stability of interconnected systems," *IEEE Trans. Autom. Control*, vol. 41, no. 3, pp. 349–357, Mar. 1996.

[11] D. Yanakiev and I. Kanellakopoulos, "Variable time headway for string stability of automated heavy-duty vehicles," in *Proc. 34th IEEE Conf. Decision Control*, New Orleans, LA, 1995, pp. 4077–4081.

[12] Y. Zhang, E. B. Kosmatopoulos, P. A. Ioannou, and C. C. Chien, "Autonomous intelligent cruise control using front and back information for tight vehicle following maneuvers," *IEEE Trans. Veh. Technol.*, vol. 48, no. 1, pp. 319–328, Jan. 1999.

Bounding the Parameters of Linear Systems With Input Backlash

V. Cerone and D. Regruto

***Abstract*—In this note we present a two-stage procedure for deriving parameters bounds of linear systems with input backlash when the output measurement errors are bounded. First, using steady-state input-output data, parameters of the nonlinear dynamic block are tightly bounded. Then, given a suitable PRBS input sequence we evaluate tight bounds on the unmeasurable inner signal which, together with noisy output measurements are employed for bounding the parameters of the linear dynamic system.**

***Index Terms*—Backlash, bounded uncertainty, errors-in-variable, output errors, parameter bounding.**

I. INTRODUCTION

Control systems components, such as sensors and actuators, often exhibits backlash which, indeed, is a typical characteristic of mechanical connections (see, e.g. [1]). Backlash (see Fig. 1) can be classified as a hard (i.e. non-differentiable) and dynamic nonlinearity. It is well known that this kind of nonlinearity may often cause delays, oscillations and inaccuracy which severely limit the performance of control systems (see, e.g. [2]). To cope with these limitations, either robust or adaptive control techniques can be successfully employed (see, e.g., [3], and [4] respectively) which, on the other hand, require the characterization of the nonlinear dynamic block. Amazingly, there are only few contributions in the literature on the identification of systems with nonstatic hard nonlinearities ([5]). Therefore, the identification of systems with unknown backlash is an open theoretical problem of major relevance to applications.

The configuration we are dealing with in this note, shown in Fig. 2, closely resembles that of a Hammerstein model which in turn consists of a static nonlinear part $\mathcal{N}$ followed by a linear dynamic system. The identification of such a model relies solely on input–output measurements, while the inner signal x_t is not assumed to be available. Identification of the Hammerstein structure has attracted the attention of many authors, as can be seen in [6] and [7]. It must be stressed that existing identification procedures mostly require that the nonlinearity be static and differantiable, usually a polynomial (see, e.g., [8]–[10] and the references therein). On the side of linear systems with hard input nonlinearities, Bai [5] considers the case of nonlinearities parameterized by one parameter. The proposed algorithm, based on the idea of separable least squares, can be applied to several common static and nonstatic input nonlinearities.

In identification, a common assumption is that the measurement error η_t is statistically described. A worthwhile alternative to the stochastic description of measurement errors is the bounded-errors characterization, where uncertainties are assumed to belong to a given set. In the bounding context, all parameter vectors belonging to the *feasible parameter set* (FPS), i.e., parameters consistent with the

Manuscript received March 14, 2005; revised January 16, 2006 and July 31, 2006. Recommended by Associate Editor J. Berg. This research was supported in part by the italian Ministero dell'Istruzione, dell'Università e della Ricerca (MIUR), under the plan "Robustness and Optimization Techniques for High Performance Control Systems."

The authors are with the Dipartimento di Automatica e Informatica, Politecnico di Torino, 10129 Torino, Italy (e-mail: vito.cerone@polito.it; diego.regruto@polito.it).

Digital Object Identifier 10.1109/TAC.2007.892375

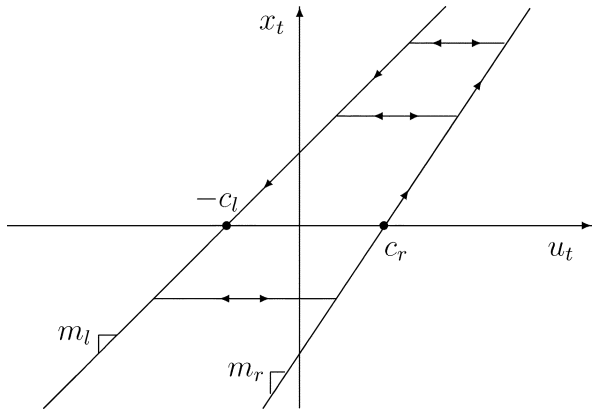

Fig. 1. Backlash.

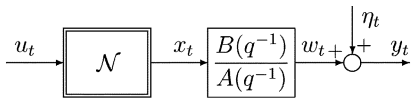

Fig. 2. SISO discrete-time linear system with input backslash $\mathcal{N}$.

measurements, the error bounds and the assumed model structure, are feasible solutions of the identification problem. The interested reader can find further details on this approach in a number of survey papers (see, e.g., [11]–[13].

In this note, we present a scheme for the identification of linear systems with input backlash. More precisely, we address the problem of bounding the parameters of a stable single-input–single-output (SISO) discrete-time linear system with unknown backlash at the input (see Fig. 2) when the output error is considered to be bounded. Note that the inner signal $x(t)$ is not supposed to be measurable. To the authors' best knowledge, no contribution can be found in the literature which address the previously described identification problem, except for the authors' work [14]. The results presented here, significantly improve paper [14], namely: a) a more general model of the backlash is considered; b) evaluation of the backlash parameters bounds and inner signal bounds does not rely any more on graphical inspection of the two-dimensional parameter space, instead a couple of optimization results are given which provide tight bounds both on parameters and unmeasurable signal for any given number of steady state measurements; and c) the simulated example has been revised accordingly. The note is organized as follows. Section II is devoted to the formulation of the problem. In Section III, parameters of the nonlinear block are tightly bounded using input-output data collected from the steady-state response of the system to a square wave input. Then, in Section IV, through a dynamic experiment, for all u_t belonging to a suitable pseudo random binary signal (PRBS) sequence $\{u_t\}$, we compute tight bounds on the inner signal which, together with noisy output measurements are used for bounding the parameters of the linear part. A simulated example is reported in Section V.

II. Problem Formulation

Consider the SISO discrete-time linear system with input backlash depicted in Fig. 2, where the nonlinear block transforms the input signal u_t into the unmeasurable inner variable x_t according to the following map (see, e.g., [2])

$$x_t = \begin{cases} m_l(u_t + c_l), & \text{for } u_t \le z_l \\ m_r(u_t - c_r), & \text{for } u_t \ge z_r \\ x_{t-1}, & \text{for } z_l < u_t < z_r \end{cases} \tag{1}$$

where $m_l > 0$, $m_r > 0$, $c_l > 0$, $c_r > 0$ are constant parameters characterizing the backlash and

$$z_l = \frac{x_{t-1}}{m_l} - c_l \quad z_r = \frac{x_{t-1}}{m_r} + c_r \tag{2}$$

are the u-axis values of intersections of the two lines, with slopes m_l and m_r, with the horizontal inner segment containing x_{t-1}. The backlash characteristics is depicted in Fig. 1. The linear dynamic part is modeled by a discrete-time system which transforms x_t into the noise-free output w_t according to the linear difference equation

$$A(q^{-1})w_t = B(q^{-1})x_t \tag{3}$$

where $A(q^{-1}) = 1 + a_1 q^{-1} + \ldots + a_{na} q^{-na}$ and $B(q^{-1}) = b_0 + b_1 q^{-1} + \ldots + b_{nb} q^{-nb}$. In line with the work done by a number of authors, in the contest of identification of block oriented systems, we assume that: i) the linear system is asymptotically stable (see, e.g., [15]–[19]); ii) $\sum_{j=0}^{nb} b_j \neq 0$, that is, the steady-state gain is not zero (see, e.g. [17]–[19]); iii) an estimate of the process settling-time (see, e.g., [20]) is available. Let y_t be the noise-corrupted output

$$y_t = w_t + \eta_t. \tag{4}$$

Measurements uncertainty is known to range within given bounds $\Delta\eta_t$, i.e.,

$$|\eta_t| \le \Delta\eta_t. \tag{5}$$

Unknown parameter vectors $\gamma \in R^4$ and $\theta \in R^p$ are defined, respectively, as

$$\gamma^T = [\gamma_1 \;\; \gamma_2 \;\; \gamma_3 \;\; \gamma_4] = [m_l \;\; c_l \;\; m_r \;\; c_r] \tag{6}$$

$$\theta^T = [a_1 \;\; \ldots \;\; a_{na} \;\; b_0 \;\; b_1 \;\; \ldots \;\; b_{nb}] \tag{7}$$

where $na + nb + 1 = p$. It is easy to show that the parameterization of the structure of Fig. 2 is not unique. To get a unique parameterization, in this work we assume, without loss of generality, that the steady-state gain of the linear part be one, that is

$$g = \frac{\sum_{j=0}^{nb} b_j}{1 + \sum_{i=1}^{na} a_i} = 1. \tag{8}$$

In this note, we address the problem of deriving bounds on parameters γ and θ consistently with given measurements, error bounds and the assumed model structure.

III. Assessment of Tight Bounds on the Nonlinear Static Block Parameters

Here, we exploit steady-state operating conditions to bound the parameters of the backlash. The noisy output sequence is collected from the steady-state response of the system to a set of square wave inputs with different amplitudes. Due to the fact that the backlash deadzone is unknown (its evaluation is the main purpose of this section) we suggest to choose the input amplitude in such a way that the output shows any nonzero response. For each value of the input square wave amplitude, only one steady-state value of the noisy output is considered on the positive half-wave of the input and one steady-state value of the noisy output on the negative half-wave. Thus, given a set of square wave inputs with M different amplitudes, $2M$ steady-state values of the output are taken into account. We only assume to have a rough idea of the settling time of the system under consideration, in order to know when steady-state conditions are reached, so that steady-state data can

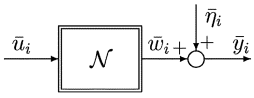

Fig. 3. Steady-state behaviour of the system under consideration when $\boldsymbol{g} = \mathbf{1}$.

be collected. Indeed, under conditions i)–iii) stated in Section II, combining (1), (3) and (4) at steady-state, we get the following input–output description involving only the parameters of the backlash:

$$\bar{y}_i = m_r(\bar{u}_i - c_r) + \bar{\eta}_i, \quad \text{for } \bar{u}_i \geq \frac{\bar{x}_{i-1}}{m_r} + c_r, \qquad i = 1, \ldots, M \tag{9}$$

$$\bar{y}_j = m_l(\bar{u}_j + c_l) + \bar{\eta}_j, \quad \text{for } \bar{u}_j \leq \frac{\bar{x}_{j-1}}{m_l} - c_l, \qquad j = 1, \ldots, M \tag{10}$$

where the triplets $\{\bar{u}_i, \bar{y}_i, \bar{\eta}_i\}$ and $\{\bar{u}_j, \bar{y}_j, \bar{\eta}_j\}$ are collections of steady-state values of the known input signal, output observation and measurement error taken during the positive and the negative square wave, respectively. A block diagram description of the steady-state response is depicted in Fig. 3 for (9) only; (10) leads to a similar block diagram representation. Since the pairs (m_l, c_l) and (m_r, c_r) affect the collected measurements, i.e., (9) and (10), separately, we can define the feasible parameter region of the backlash as

$$\mathcal{D}_\gamma = \mathcal{D}_\gamma^r \bigcup \mathcal{D}_\gamma^l \tag{11}$$

where

$$\mathcal{D}_\gamma^r = \left\{ m_r, c_r \in R^+ : \bar{y}_i = m_r(\bar{u}_i - c_r) + \bar{\eta}_i, \; |\bar{\eta}_i| \leq \Delta\bar{\eta}_i, \; i = 1, \ldots, M \right\} \tag{12}$$

$$\mathcal{D}_\gamma^l = \left\{ m_l, c_l \in R^+ : \bar{y}_j = m_l(\bar{u}_j + c_l) + \bar{\eta}_j, \; |\bar{\eta}_j| \leq \Delta\bar{\eta}_j, \; j = 1, \ldots, M \right\} \tag{13}$$

where $\{\Delta\bar{\eta}_i\}$ and $\{\Delta\bar{\eta}_j\}$ are the sequences of bounds on measurements uncertainty. From definition (11) it can be seen that $\mathcal{D}_\gamma$ is exactly described by the following constraints in the parameter space:

$$\begin{aligned} \bar{y}_i - m_r(\bar{u}_i - c_r) &\geq -\Delta\bar{\eta}_i \\ \bar{y}_i - m_r(\bar{u}_i - c_r) &\leq \Delta\bar{\eta}_i, \; m_r > 0, c_r > 0, \\ & i = 1, \ldots, M \end{aligned} \tag{14}$$

$$\begin{aligned} \bar{y}_j - m_l(\bar{u}_j + c_l) &\geq -\Delta\bar{\eta}_j \\ \bar{y}_j - m_l(\bar{u}_j + c_l) &\leq \Delta\bar{\eta}_j, \; m_l > 0, c_l > 0, \\ & j = 1, \ldots, M. \end{aligned} \tag{15}$$

Remark 1: $\mathcal{D}_\gamma^l$ and $\mathcal{D}_\gamma^r$ are two-dimensional sets lying on the (m_l, c_l)-plane and the (m_r, c_r)-plane, respectively, i.e., they are disjoint sets, which means that they can be handled separately. We also note that they have the same mathematical structure, which means that they enjoy the same properties. Thus, from here on the results derived for one of the two sets, say $\mathcal{D}_\gamma^r$, will be also applicable to the other set $(\mathcal{D}_\gamma^l)$. Throughout this note, it is assumed that $\mathcal{D}_\gamma^r$ $(\mathcal{D}_\gamma^l)$ is a bounded set: To this end it suffices to collect at least two sets of measurements with different inputs u. Here, we present some possible descriptions of the feasible parameter set $\mathcal{D}_\gamma^r$. Introductory definitions and preliminary results are first given.

A. Definitions and Preliminary Results

Definition 1: $h_r^+(\overline{u}_s)$ and $h_r^-(\overline{u}_s)$ are the constraints boundaries defining the FPS $\mathcal{D}_\gamma^r$ corresponding to the sth sets of data

$$h_r^+(\overline{u}_s) \doteq \left\{ m_r \in R^+, c_r \in R^+ : \overline{y}_s + \Delta\eta_s = m_r(\overline{u}_s - c_r) \right\}$$

$$h_r^-(\overline{u}_s) \doteq \left\{ m_r \in R^+, c_r \in R^+ : \overline{y}_s - \Delta\eta_s = m_r(\overline{u}_s - c_r) \right\}.$$

Definition 2: Boundary of $\mathcal{D}_\gamma^r \doteq \mathcal{H}(\mathcal{D}_\gamma^r)$.

Definition 3: The constraints boundaries $h_r^+(\overline{u}_s)$ and $h_r^-(\overline{u}_s)$ are said to be active if their intersections with $\mathcal{H}(\mathcal{D}_\gamma^r)$ is not the empty set

$$h_r^+(\overline{u}_s) \bigcap \mathcal{H}\left(\mathcal{D}_\gamma^r\right) \neq \emptyset \Longleftrightarrow h_r^+(\overline{u}_s) \text{ is active}$$

$$h_r^-(\overline{u}_s) \bigcap \mathcal{H}\left(\mathcal{D}_\gamma^r\right) \neq \emptyset \Longleftrightarrow h_r^-(\overline{u}_s) \text{ is active.}$$

Remark 2: It is trivial to see that the constraints boundaries $h_r^+(\overline{u}_s)$ and $h_r^-(\overline{u}_s)$ may either: a) intersect $\mathcal{H}(\mathcal{D}_\gamma^r)$, or b) be external to $\mathcal{H}(\mathcal{D}_\gamma^r)$, hence, be external to $\mathcal{D}_\gamma^r$.

Definition 4: Edges of $\mathcal{D}_\gamma^r$

$$\begin{aligned} \tilde{h}_r^+(\overline{u}_s) &\doteq h_r^+(\overline{u}_s) \bigcap \mathcal{D}_\gamma^r \\ &= \left\{ m_r, c_r \in \mathcal{D}_\gamma^r : \overline{y}_s + \Delta\eta_s = m_r(\overline{u}_s - c_r) \right\} \\ \tilde{h}_r^-(\overline{u}_s) &\doteq h_r^-(\overline{u}_s) \bigcap \mathcal{D}_\gamma^r \\ &= \left\{ m_r, c_r \in \mathcal{D}_\gamma^r : \overline{y}_s - \Delta\eta_s = m_r(\overline{u}_s - c_r) \right\}. \end{aligned}$$

Definition 5: Constraints intersections. The set of all the pairs $(m_r, c_r) \in R^2$ where intersections among the constraints occur is

$$\mathcal{I}_\gamma^r = \left\{ (m_r, c_r) \in R^2 : \left\{ h_r^+(\overline{u}_i), h_r^-(\overline{u}_i) \right\} \bigcap \left\{ h_r^+(\overline{u}_j), h_r^-(\overline{u}_j) \right\} \neq \emptyset; i, j = 1, \ldots, M; i \neq j \right\}. \tag{16}$$

Definition 6: Vertices of $\mathcal{D}_\gamma^r$. The set of all the vertices of $\mathcal{D}_\gamma^r$ is defined as the set of all the intersection couples belonging to the feasible parameter set $\mathcal{D}_\gamma^r$

$$\mathcal{V}\left(\mathcal{D}_\gamma^r\right) = \mathcal{I}_\gamma^r \bigcap \mathcal{D}_\gamma^r. \tag{17}$$

B. Exact Description of $\mathcal{D}_\gamma^r$

An exact description of $\mathcal{D}_\gamma^r$ can be given in terms of edges, each one being described, from a practical point of view, as a subset of an active constraint lying between two vertices. An effective procedure for deriving active constraints, vertices and edges of $\mathcal{D}_\gamma^r$ is reported in the Appendix.

C. Tight Orthotope Description of $\mathcal{D}_\gamma^r$

Edges provide exact description of $\mathcal{D}_\gamma^r$ which, on the downside, could be not so easy to handle. A somewhat more practical description, although approximate, can be obtained by the computation of the following orthotope outer-bounding set $\mathcal{B}_\gamma^r$ tightly containing $\mathcal{D}_\gamma^r$:

$$\mathcal{B}_\gamma^r = \left\{ \gamma \in R^2 : \gamma_j = \gamma_j^c + \delta\gamma_j, |\delta\gamma_j| \leq \Delta\gamma_j, \; j = 1, 2 \right\} \tag{18}$$

where

$$\gamma_j^c = \frac{\gamma_j^{\min} + \gamma_j^{\max}}{2} \qquad \Delta\gamma_j = \frac{\left|\gamma_j^{\max} - \gamma_j^{\min}\right|}{2} \tag{19}$$

$$\gamma_j^{min} = \min_{\gamma \in \mathcal{D}_\gamma^r} \gamma_j \qquad \gamma_j^{\max} = \max_{\gamma \in \mathcal{D}_\gamma^r} \gamma_j. \tag{20}$$

Since constraints (15) defining $\mathcal{D}_\gamma$ are nonlinear in m_r and c_r, at least in principle the solution of the previous optimization problems (20) requires the use of nonconvex optimization techniques which, however, do not guarantee the finding of the global optimal solution. Problems (20) can be solved thanks to the result reported later.

Proposition 1: The global optimal solutions of problems (20) occur on the vertices of $\mathcal{D}_\gamma^r$.

Proof: First, i) we notice that each level curve of functionals (20)—parallel lines to m_r-axis and c_r-axis respectively—intersect the boundary of each constraint in (15) only once. Next, ii) objective functions in (20) are monotone which implies that the optimal solution lies on the boundary of $\mathcal{D}_\gamma^r$. Thanks to i), the optimal value cannot lie on one edge between two vertices: if that was true, it would mean that there is

a suboptimal value where the functional intersect the edge twice: That would contradict i). Then the global optimal solutions of problems (20) can only occur on the vertices of $\mathcal{D}_\gamma^r$.

Remark 3: Given the set of vertices $\mathcal{V}(\mathcal{D}_\gamma^r)$ computed via the procedure of the Appendix, the evaluation of (20) is an easy task since it only requires the calculation of a) the objective functions on a set of points $\leq 4M$ and b) the maximum over a set of real values.

IV. Bounding the Parameters of the Linear Dynamic Model

In the second stage of our procedure, we evaluate bounds on the parameters of the linear dynamic block. In this stage, we excite the system to be identified with a PRBS which takes the values $\pm u^\star$. We recall that, thanks to its nice properties, a PRBS input is successfully employed in linear system identification [21], [22]. Although PRBS inputs are not suitable for nonlinear system identification in general [5], [23] since it may not adequately excite the unknown nonlinearity, in [24] it is shown that such a signal can be effectively used to decouple the linear and nonlinear parts in the identification of Hammerstein model with static nonlinearity. In this note we show that the use of a PRBS sequence is profitable for the identification of linear system with input backlash. The key idea underlying our contribution is based on the following result.

Result 1: Under a PRBS input whose levels are $\pm u^\star$, $u^\star > c_r$ and $-u^\star < -c_l$, the output of a backlash described by (1) is still a PRBS with levels $\bar{x}^\star = m_r(u^\star - c_r)$, $\underline{x}^\star = m_l(u^\star - c_l)$.

The proof of Result 1 is not reported since it is a trivial one.

Given the exact description of $\mathcal{D}_\gamma^r$, tight bounds on the magnitude $\bar{x}^\star$ of the unmeasurable pseudo random inner signal x_t can be computed $\forall t$ through the following expressions

$$\begin{aligned} \bar{x}^{\star min} &= \min_{m_r, c_r \in \mathcal{D}_\gamma^r} m_r(u^\star - c_r), \quad \text{for } u^\star \geq c_r \\ \bar{x}^{\star max} &= \max_{m_r, c_r \in \mathcal{D}_\gamma^r} m_r(u^\star - c_r), \quad \text{for } u^\star \geq c_r. \end{aligned} \tag{21}$$

Computation of bounds in (21) requires, at least in principle, the solution of two nonconvex optimization problems with two variables and $4M$ constraints. However, the computational efforts can be dramatically reduced thanks to the results reported later, where we exploit the following definition.

Definition 7: x-level curve of the objective function to be optimized

$$g_r(u^\star, x) \doteq \left\{ m_r \in R^+, c_r \in R^+ : x = m_r(u^\star - c_r) \right\}. \tag{22}$$

Proposition 2: The global optimal solutions of problems (21) occur on the vertices of $\mathcal{D}_\gamma^r$.

Proof: First, i) we notice that the each x-level curve $g_r(u^\star, x)$ intersect each constraint boundary in (15) only once. Next, ii) the objective function (22) is a monotone function which implies that the optimal solution lies on the boundary of $\mathcal{D}_\gamma^r$. Thanks to i) the optimal value cannot lie on an edge between two vertices: If that was true, it would mean that there is a suboptimal value where the functional intersect the edge twice: That would contradict i). Then the global optimal solutions of problems (21) can only occur on the vertices of $\mathcal{D}_\gamma^r$.

Here, same comments as *Remark 3* apply.

Now, if we define the quantities

$$x_t^c = \frac{\bar{x}^{\star min} + \bar{x}^{\star max}}{2} \qquad \Delta x_t = \frac{\bar{x}^{\star max} - \bar{x}^{\star min}}{2} \tag{23}$$

the following relation can be established between the unknown inner signal x_t and the central value x_t^c:

$$x_t^c = x_t + \delta x_t \tag{24}$$

$$|\delta x_t| \leq \Delta x_t. \tag{25}$$

We can now formulate the identification of the linear model in terms of the noisy output sequence $\{y_t\}$ and the uncertain inner sequence $\{x_t^c\}$ as shown in Fig. 4. Such a formulation is commonly referred to as an errors-in-variables (EIV) problem, i.e., a parameter estimation problem in a linear-in-parameter model where the output and some or all the explanatory variables are uncertain. This stage of the procedure is quite standard and it will not be discussed in the note. The interested readers can find the details in [9], [14], and [25].

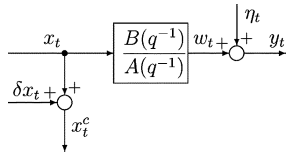

Fig. 4. EIV setup for bounding the parameters of the linear system.

Remark 4: A possible limitation of the proposed approach is that the identification of the linear system relies on computed bounds of the inner signal which, in turn, depends on the accuracy of the backlash parameter estimates. However, it must be pointed out that both the backlash feasible parameter set and inner signal bounds are tightly computed, thus no conservatism is introduced in the proposed procedure.

V. A Simulated Example

In this section, we illustrate the proposed parameter bounding procedure through a numerical example. The system considered here is characterized by a linear block with $A(q^{-1}) = (1 + 0.5q^{-1} - 0.1q^{-2})$ and $B(q^{-1}) = (0.2q^{-1} + 1.2q^{-2})$ and a nonsymmetric backlash with $m_l = 0.24$, $m_r = 0.26$, $c_l = 0.035$, $c_r = 0.070$. Thus, the true parameter vectors are $\gamma = [m_l\ c_l\ m_r\ c_r]^{\mathrm{T}} = [0.24\ 0.035\ 0.26\ 0.070]^{\mathrm{T}}$ and $\theta = [a_1\ a_2\ b_1\ b_2]^{\mathrm{T}} = [0.5\ -0.1\ 0.2\ 1.2]^{\mathrm{T}}$. We emphasize that the backlash parameters have been realistically chosen: as a matter of fact we considered the parameters of a real world precision gearbox which features a gear ratio equal to 0.25 and a deadzone as low as 0.0524 rad ($\approx 3^o$) and simulated a possible fictitious nonsymmetric backlash with gear ratio $m_l = 0.24$, $m_r = 0.26$ and deadzone $c_l = 0.035$ ($\approx 2^o$), $c_r = 0.070$ ($\approx 4^o$). Bounded absolute output errors have been considered when simulating the collection of both steady state data, $\{\bar{u}_s, \bar{y}_s\}$, and transient sequence $\{u_t, y_t\}$. Here we assumed $|\eta_t| \leq \Delta\eta_t$ and $|\bar{\eta}_s| \leq \Delta\bar{\eta}_s$ where η_t and $\bar{\eta}_s$, are random sequences belonging to the uniform distributions $U[-\Delta\eta_t, +\Delta\eta_t]$ and $U[-\Delta\bar{\eta}_s, +\Delta\bar{\eta}_s]$ respectively. Bounds on steady-state and transient output measurement errors were supposed to have the same value, i.e., $\Delta\eta_t = \Delta\bar{\eta}_s \doteq \Delta\eta$. Eight different values of $\Delta\eta$ were chosen in such a way as to simulate the measurement errors of eight commercial absolute binary encoder with a number of bits n_{bit} varying from 8 to 15. For a given $\Delta\eta$, the length of steady-state and the transient data are $M = 50$ and $N = [100, 1000]$, respectively. The steady-state input samples $\bar{u}_s$ are equally spaced values from 0.6 and 3, while the transient input sequence $\{u_t\}$ is a PRBS which takes the values ± 1. Results about the nonlinear and the linear block are reported in Figs. 5–7, respectively. For low noise level ($n_{bit} > 10$ bits) and for all N, the central estimates of both the nonlinear static block and the linear model are consistent with the true parameters. For higher noise levels ($n_{bit} \leq 10$ bits), both $\gamma^c = [m^c, c^c]$ and θ^c give satisfactory estimates of the true parameters. As the number of observations increases (from $N = 100$ to $N = 1000$), parameter uncertainty bounds $\Delta\theta_j$ decreases, as expected.

VI. Conclusion

A two-stage parameter bounding procedure for linear systems with input backlash in presence of bounded output errors has been outlined. First, using steady-state input–output data the two parameters of the

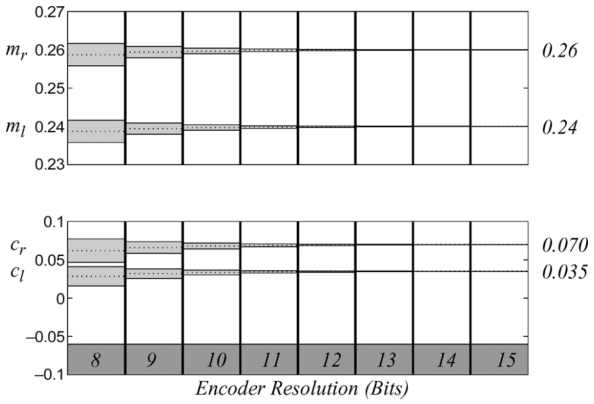

Fig. 5. Backlash parameter identification: central estimates (dotted) and parameters uncertainty intervals (shaded) versus encoder resolution $(\boldsymbol{M = 50})$.

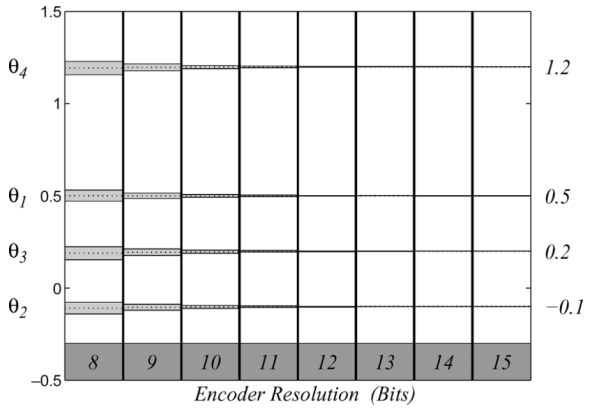

Fig. 6. Linear system parameter identification: central estimates (dotted) and parameters uncertainty intervals (shaded) versus encoder resolution $(\boldsymbol{N = 100})$.

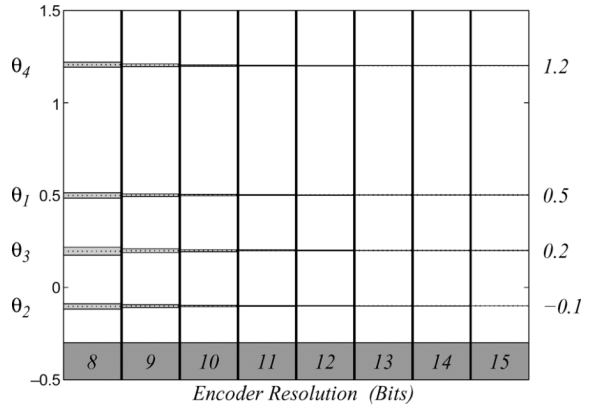

Fig. 7. Linear system parameter identification: central estimates (dotted) and parameters uncertainty intervals (shaded) versus encoder resolution $(\boldsymbol{N = 1000})$.

backlash have been tightly bounded. Then, for a given input transient sequence we have computed bounds on the unmeasurable inner signal which, together with output noisy measurements have been used to overbound the parameters of the linear part. The numerical example showed the effectiveness of the proposed procedure.

APPENDIX

In this appendix, the procedure for the computation of vertexes and active constraints defining the feasible parameter set $\mathcal{D}_\gamma^r$ is presented. In order to simplify the presentation of the algorithm, the symbol $\mathcal{V}$ is used instead of $\mathcal{V}(\mathcal{D}_\gamma^r)$ and the following additional symbols and quantities are introduced: H_L is a list of active constraints boundaries, that is, each element $H_L(k)$ of the list is an active constraint boundary; the expression $X \leftarrow \{z\}$ means that the element z is included in the set or list X; $\mathcal{D}_\gamma^r(s)$ is the set of all the parameter of the backlash which are consistent with the first s measurement, the error bound and the assumed backlash model structure. A formal description of $\mathcal{D}_\gamma^r(s)$ is

$$\mathcal{D}_\gamma^r(s) = \big\{ m_r, c_r \in R^+ : \bar{y}_i = m_r(\bar{u}_i - c_r) + \bar{\eta}_i \quad |\bar{\eta}_i| \le \Delta\bar{\eta}_i,\ i = 1, \ldots, s \big\} \tag{26}$$

The proposed procedure (see the Algorithm that follows) works in four stages. First, the active constraints boundaries and the vertexes of the set $\mathcal{D}_\gamma^r(2)$ are characterized exploiting Definitions 1, 3, 5, and 6 of Section III. Then, for each new measurement $\overline{u}_s$, all the intersections among the constraints boundaries $h^+(\overline{u}_s)$ and $h^-(\overline{u}_s)$ and the active constraints boundaries contained in the list H_L are computed; all such intersections are temporarily included in the set $\mathcal{V}$; the constraints boundaries $h^+(\overline{u}_s)$ and $h^-(\overline{u}_s)$ are included in the list H_L. Further, the vertexes of $\mathcal{D}_\gamma^r(s)$ are obtained rejecting the constraints boundaries intersections which do not satisfy all the constraints generated by the first s measurements (which implicitly defined $\mathcal{D}_\gamma^r(s)$). Finally, the list of active constraints boundaries H_L is updated retaining only the constraints boundaries whose intersection is a vertex of $\mathcal{D}_\gamma^r(s)$.

Algorithm

(Computation of vertexes and active constraints of $\mathcal{D}_\gamma^r$)

begin
$\mathcal{V} \leftarrow \{h^+(\overline{u}_1) \bigcap h^+(\overline{u}_1)\}$.
$\mathcal{V} \leftarrow \{h^+(\overline{u}_1) \bigcap h^-(\overline{u}_2)\}$.
$\mathcal{V} \leftarrow \{h^-(\overline{u}_1) \bigcap h^+(\overline{u}_2)\}$.
$\mathcal{V} \leftarrow \{h^-(\overline{u}_1) \bigcap h^-(\overline{u}_2)\}$.
$H_L \leftarrow \{h^+(\overline{u}_1), h^+(\overline{u}_2), h^-(\overline{u}_1), h^-(\overline{u}_2)\}$.
for $s = 3 : 1 : M$
  $L = \texttt{length}(H_L)$;
  $q = 0$;
  for} $z = 1 : 1 : L$
    $\mathcal{V} \leftarrow \{h^+(\overline{u}_s) \bigcap H_L(z)\}$.
    If $h^+(\overline{u}_s) \notin H_L$ **then**
      $H_L \leftarrow \{h^+(\overline{u}_s)\}$.
    end if
    $\mathcal{V} \leftarrow \{h^-(\overline{u}_s) \bigcap H_L(z)\}$.
    If $h^-(\overline{u}_s) \notin H_L$ **then**
      $H_L \leftarrow \{h^-(\overline{u}_s)\}$.
    end if
  end for
  $\mathcal{V} = \{\mathcal{V} \bigcap \mathcal{D}_\gamma^r(s)\}$.
  for $k = 1 : 1 : \texttt{length}(H_L)$
    If $\exists j \neq k : \{H_L(k) \bigcap H_L(j)\} \in \mathcal{V}$ **then**
      $H_{aux}(q) = H_L(k)$.
      $q = q + 1$.
    end if
  end for
$H_L = H_{aux}$.
end for
return H_L.
return $\mathcal{V}$.
end

REFERENCES

[1] M. Nordin and P. O. Gutman, "Controlling mechanical systems with backlash—A survey," *Automatica*, vol. 38, pp. 1633–1649, 2002.

[2] G. Tao and P. Kokotovic*, Adaptive Control of Systems With Actuator and Sensor Nonlinearities*. New York: Wiley, 1996.

[3] M. Corradini, G. Orlando, and G. Parlangeli, "A VSC approach for the robust stabilization of nonlinear plants with uncertain nonsmooth actuator nonlinearities—A unified framework," *IEEE Trans. Autom. Control*, vol. 49, no. 5, pp. 807–813, May 2004.

[4] G. Tao and C. Canudas de Wit, Eds., "Special issue on adaptive systems with non-smooth nonlinearities," *Int. J. Adapt. Control Signal Process.*, vol. 11, no. 1, 1997.

[5] E. Bai, "Identification of linear systems with hard input nonlinearities of known structure," *Automatica*, vol. 38, pp. 853–860, 2002.

[6] S. Billings, "Identification of nonlinear systems—A survey," *Proc. Inst. Elect. Eng. D*, vol. 127, no. 6, pp. 272–285, 1980.

[7] R. Haber and H. Unbehauen, "Structure identification of nonlinear dynamic systems—A survey on input/output approaches," *Automatica*, vol. 26, no. 4, pp. 651–677, 1990.

[8] E. Bai, "An optimal two-stage identification algorithm for Hammerstein-Wiener nonlinear systems," *Automatica*, vol. 34, no. 3, pp. 333–338, 1998.

[9] V. Cerone and D. Regruto, "Parameter bounds for discrete time Hammerstein models with bounded output errors," *IEEE Trans. Autom. Control*, vol. 48, no. 10, pp. 1855–1860, Oct. 2003.

[10] K. Narendra and P. Gallman, "An iterative method for the identification of nonlinear systems using a Hammerstein model," *IEEE Trans. Autom. Control*, vol. AC-11, no. 3, pp. 546–550, Jul. 1966.

[11] M. Milanese and A. Vicino, "Optimal estimation theory for dynamic sistems with set membership uncertainty: An overview," *Automatica*, vol. 27, no. 6, pp. 997–1009, 1991.

[12] E. Walter and H. Piet-Lahanier, "Estimation of parameter bounds from bounded-error data: A survey," *Math. Comput. Simul.*, vol. 32, pp. 449–468, 1990.

[13] M. Milanese, J. Norton, H. Piet-Lahanier, and E. Walter, Eds., *Bounding Approaches to System Identification*. New York: Plenum, 1996.

[14] V. Cerone and D. Regruto, "Bounding the parameters of linear systems with input backlash," in *Proc. Amer. Control Conf.*, 2005, pp. 4476–4481.

[15] P. Stoica and T. Söderström, "Instrumental-variable methods for identification of Hammerstein systems," *Int. J. Control*, vol. 35, no. 3, pp. 459–476, 1982.

[16] A. Krzyżak, "Identification of nonlinear block-oriented systems by the recursive kernel estimate," *Int. J. Franklin Inst.*, vol. 330, no. 3, pp. 605–627, 1993.

[17] Z. Lang, "Controller design oriented model identification method for Hammerstein system," *Automatica*, vol. 29, no. 3, pp. 767–771, 1993.

[18] ——, "A nonparametric polynomial identification algorithm for the Hammerstein system," *IEEE Trans. Autom. Control*, vol. 42, no. 10, pp. 1435–1441, Oct. 1997.

[19] L. Sun, W. Liu, and A. Sano, "Identification of a dynamical system with input nonlinearity," *Proc. Inst. Elect. Eng. D*, vol. 146, no. 1, pp. 41–51, 1999.

[20] A. Kalafatis, L. Wang, and W. Cluett, "Identification of Wiener-type nonlinear systems in a noisy enviroment," *Int. J. Control*, vol. 66, no. 6, pp. 923–941, 1997.

[21] L. Ljung*, System Identification, Theory for the User*. Upper Saddle River, NJ: Prentince-Hall, 1999.

[22] T. Söderström and P. Stoica*, System Identification*. Upper Saddle River, NJ: Prentice-Hall, 1989.

[23] B. Ninness and S. Gibson, "Quantifying the accuracy of Hammerstein model estimation," *Automatica*, vol. 38, pp. 2037–2051, 2002.

[24] E. Bai, "Decoupling the linear and nonlinear parts in Hammerstein model identification," *Automatica*, vol. 40, no. 4, pp. 671–676, 2004.

[25] V. Cerone, "Feasible parameter set for linear models with bounded errors in all variable," *Automatica*, vol. 29, no. 6, pp. 1551–1555, 1993.

Closed-Loop Behavior of a Class of Nonlinear Systems Under EKF-Based Control

Jeffrey H. Ahrens and Hassan K. Khalil

***Abstract*—We study the closed-loop behavior of the extended Kalman filter (EKF) for a class of deterministic nonlinear systems that are transformable to the special normal form with linear internal dynamics. We argue that the closed-loop system is asymptotically stable and the estimation error exponentially converges to zero. We compare the performance of the EKF to a high-gain observer through simulation.**

***Index Terms*—Kalman filtering, nonlinear control, observers, output feedback control, singular perturbation.**

I. INTRODUCTION

Since the 1970s, the extended Kalman flter (EKF) has seen successful applications as a state estimator for nonlinear stochastic systems [9], [18]. In the noise free case, the EKF can be parameterized to function as an observer for deterministic nonlinear systems. Stability and convergence properties were studied in the 1990s. An early method for constructing deterministic observers as asymptotic limits of filters appeared in [3]. Additional work on the convergence properties of extended Kalman filters used as observers has been conducted in [4], [5], [8], and [15]–[17]. Early convergence results showed that the EKF converges exponentially for general classes of systems, but these results were mostly local. Efforts to expand the domain of attraction appeared in [4] and [15]. In [8], it was recognized that, for a particular parameterization of the covariance matrices, the EKF is a time-varying high-gain observer that asymptotically approaches a fixed gain observer as the gain is pushed higher. Furthermore, it was shown that the EKF is a global exponential observer for a class of nonlinear systems transformable to the lower triangular form. This argument was based on a global Lipschitz property for the system nonlinearities.

To this point, analysis of the closed-loop system under EKF feedback has been limited. A separation result for a Kalman-like observer for a certain class of multiple-input–multiple-output (MIMO) nonlinear systems was presented in [20]. It assumed boundedness of the states of the closed-loop system and gave global results under global Lipschitz conditions. Aside from very restrictive assumptions on the nonlinearities, exponential stability of the estimation error does not guarantee the behavior of the closed-loop system, even when the system under state feedback is exponentially stable [19]. Hence, it seems appropriate to study the behavior of the closed-loop system when an extended Kalman filter is used as an observer. Toward that end, we relax the global Lipschitz condition and consider a class of systems transformable to the special normal form with linear internal dynamics. Based on a parameterization of the Riccati equation, the closed-loop system under EKF feedback is placed in the standard singularly perturbed form. We note that by relaxing the global Lipschitz condition, difficulties may arise as a result of the peaking phenomenon. Peaking in the estimates can

Manuscript received November 7, 2005; revised August 26, 2006. Recommended by Associate Editor L. Magni. This work was supported in part by the National Science Foundation under Grants ECS-0114691 and ECS-0400470.

The authors are with the Department of Electrical and Computer Engineering, Michigan State University, East Lansing, MI 48824-1226 USA (e-mail: ahrensj1@egr.msu.edu; khalil@egr.msu.edu).

Color versions of one or more of the figures in this paper are available online at http://ieeexplore.ieee.org.

Digital Object Identifier 10.1109/TAC.2007.892376